

Performance of continuous time quantum walks under phase damping

J. Lockhart,¹ C. Di Franco,² and M. Paternostro²

¹*School of Electronics, Electrical Engineering and Computer Science,
Queen's University, Belfast, BT7 1NN, United Kingdom*

²*Centre for Theoretical Atomic, Molecular and Optical Physics,
School of Mathematics and Physics, Queen's University, Belfast, BT7 1NN, United Kingdom*

We study the resilience to decoherence of the glued trees continuous time algorithm described by Childs *et al.* in [1]. We consider a discrete time reformulation of the problem and apply a phase damping channel to the coin state, studying the effect of such a mechanism on the probability of the walker appearing on the target vertex of the graph. We pay particular attention to any potential advantage coming from the use of weak decoherence for the spreading of the walker across the glued trees graph.

Arguably the main hindrance to the grounding of a platform for quantum technologies is the effect of noise or “decoherence” on quantum states. No physical system is ever truly closed and will interact with its environment. As a result of such interaction, the quantum state of the system will approach classicality, thus ceasing to be of interest for quantum-empowered protocols [2]. Before we are to create useful quantum technologies, these processes will need to be understood, and eventually controlled.

An intriguing aspect of decoherence is that, in specific cases (such as quantum stochastic resonances, to throw an example), weak decoherence mechanisms give rise to sizeable advantages in, say, the performance of some quantum protocols or the transport of excitations across a quantum medium. Such counterintuitive effects are tightly linked to quantum interference phenomena: the occurrence of decoherence changes the way the wave function of a given system evolves in time, thus affecting the occurrence of constructive and destructive interference. “Accidental” constructive effects may be induced, without spoiling the working principle of a given quantum process, for sufficiently weak decoherence mechanisms.

All this is particularly important (and evident) in the quantum walk framework [4], whose advantage in terms of the spreading rate of the position of a walker on a given “path” may be magnified by small degrees of phase noise [9]. In this paper we contribute to the ongoing research in this context by studying the glued trees (GT) traversal algorithm described in [1] when phase-damping effects [2] are included in the otherwise unitary dynamics.

After quickly revisiting the paradigm of quantum walks, we proceed to discuss the protocol in [1], introducing phase noise and addressing the performance of the protocol for various strengths of such mechanisms.

I. QUANTUM WALKS

A quantum walk is best described as the quantum analogue of the classical random walk, although unlike the classical random walk, the evolution of a quantum walk is completely deterministic. We of course allow for super-

position states of the quantum walker, enabling the walks to exhibit interesting behaviours not shown by their classical counterparts. An comprehensive survey of quantum walks, covering both continuous and discrete time variants and detailing the behaviours of quantum walks on various structures can be found in [4]. In this paper, we focus on discrete time quantum walks.

A quantum walk operates within the Hilbert space $H = H_p \otimes H_c$, where H_p , known as the position space, describes the position of the walker on whichever structure we have it walk on (in this paper we shall refer to the structure on which a walk evolves as its *terrain*) and H_c , known as the coin space, describes an additional degree of freedom affecting the evolution of the walker: this degree of freedom determines the walker’s behaviour in the next time step. For the evolution of the walk, we define two operators: the shift operator, S and the coin operator, C . The shift operator acts on the position space of the walker, it will “move” the walker on to a new part of its terrain (for example, if the terrain of a walk is a graph, and walker is on some vertex, the shift operator will move it along an edge to another vertex), dependent on the coin state. The coin operator is analogous to the flipping of a coin in a classical random walk, it will act on the coin space which in turn affects how the walker shall evolve in its terrain when the shift operator is applied. We move the walker along by one step by applying the coin operator followed by the shift operator, thus the state of the walker after t total steps after starting in some initial state $|\psi(0)\rangle$ is described by the following

$$|\psi(t)\rangle = [S(I_p \otimes C)]^t |\psi(0)\rangle$$

where I_p is the identity operator on the position space of the walker. In other words, we apply the coin operator and the shift operator t times to the initial walker state.

In order to provide a complete view on the main features of the walk protocol, we now give some concrete examples of quantum walks.

A. Discrete time quantum walk on a line

To represent the walk terrain, the line, we shall use the set of integers. The walker can be anywhere on the line, so we give H_p the basis $\{|i\rangle : i \in \mathbb{Z}\}$. As previously described, each step of the walk involves a coin flip and a shift. In the walk on the line, the walker has a ‘‘choice’’ of two directions, left and right. In the classical random walk, the decision of which direction to walk in at each step is reached by flipping a fair coin. Likewise, in our quantum walk we shall use a coin space of degree two, viz. H_c is given the basis $\{|0\rangle, |1\rangle\}$.

We decide to use the Hadamard operator for our coin, as per [4]. This has the effect of putting our walker into a superposition of coin states and will allow for interference to occur during the course of the evolution of the walk.

The classical random walk will move one step to the left or one step to the right depending on the most recent coin flip. The same idea applies for the quantum walk. We define the shift operator like so

$$S|p, c\rangle = \begin{cases} |p-1, c\rangle, & \text{if } c = 0 \\ |p+1, c\rangle, & \text{if } c = 1 \end{cases}$$

Ambainis *et al.* have shown in [5] that the quantum walk on the line spreads out quadratically faster than the the classical random walk on the line.

B. Discrete time quantum walk on a k -regular graph

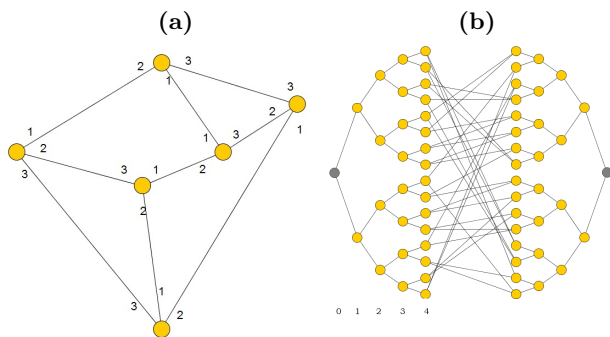


FIG. 1: (a) A labelled 3-regular graph. (b) A glued trees graph with 4 layers, $G'n$.

In general, a graph $G = (V, E)$ is specified by fixing a set of vertices V along with a set of edges E connecting them. We can make the graph k -regular by attaching k edges to each vertex. We affix a label $0 < l \leq k$ to each end of each edge, as illustrated in Fig. 1 (a). The walker will traverse the graph’s vertices, moving along the edges, so we define the position space H_p as having the basis $\{|p\rangle : p \in V\}$.

At each time step, the walker has a fan-out of k vertices to move to and we thus have to use an iso-dimensional coin space. We now give H_c the basis $\{|c\rangle : 0 < c \leq k\}$. We then introduce the Grover coin

$$C_{i,j}^{(G)} = \begin{cases} a, & \text{if } \delta_{i,j} = 0 \\ b, & \text{otherwise} \end{cases}, \quad (a, b \in \mathbb{R}) \quad (1)$$

which generalises the Hadamard coin to Hilbert spaces of dimension larger than 2 [4]. The values of a and b can be changed to vary the behaviour of the walk on the graph. We shall use a Grover coin later on to perform the simulations at the core of our work.

As for the shift operator, this must take the walker along the appropriate edge to a new vertex, depending on the coin state. Again, we state that this idea is a generalisation of the walk on the line in which we give the walker a choice of k directions at each step rather than 2. We define our shift operator like so, where c' is the label assigned to the destination node’s end of the edge

$$S|v, c\rangle = \begin{cases} |w, c'\rangle, & \text{for } (v, w) \in G \text{ and is labelled} \\ & c \text{ on } v\text{'s end,} \\ 0 & \text{otherwise.} \end{cases} \quad (2)$$

II. MODEL USED

The goal of Childs algorithm for quantum search is the following: beginning from the left-most vertex of a given glued trees graph, traverse the graph and reach the right-most vertex, referred to as the target vertex. Childs *et al.* use this algorithm to show quantum walk search to be fundamentally more effective than classical random walk search by presenting a class of graphs (the glued trees graphs) that force classical random walks to make exponentially many queries to an oracle encoding the structure of the graph, but that are traversable by quantum walks with a polynomial number of queries to such an oracle. In order to study the robustness of the algorithm to the detrimental effects of decoherence, we shall determine how effectively it achieves its goal when subjected to an increasing degree of phase damping noise. To this end, we will focus on the probability that the walker is on the target vertex at the end of the walk. We thus consider GT graphs such as the one illustrated in Fig. 1 (b), i.e. consisting of n layers before the gluing stage, and thus labelled as $G'n$.

The continuous time quantum walk can be reformulated as a discrete-time one by means of a shift operator (analogous to the one that has been previously described), and a Grover coin with $a = -1/3$ and $b = 2/3$ [3]. More explicitly

$$C^{(G)} = \frac{1}{3} \begin{pmatrix} -1 & 2 & 2 \\ 2 & -1 & 2 \\ 2 & 2 & -1 \end{pmatrix}. \quad (3)$$

We shall use this discrete-time reformulation of the protocol by Childs *et al.* to study its behaviour when affected by phase damping decoherence. The GT graphs described in [1] can straightforwardly be converted to 3-regular graphs by adding two self loops (one each to the left-most and right-most vertices), thus allowing us to use the discrete time walk model described in Sec. IB. To model decoherence we use the Kraus operators for a phase damping channel acting on the D -dimensional system embodied by the coin only [6, 7]. This modifies the initial density matrix $\rho(0)$ of a system as [2]

$$\mathcal{E}[\rho(t)] = \sum_k \hat{E}_k(t) \rho(0) \hat{E}_k^\dagger(t), \quad (4)$$

where we have introduced the Kraus operators for phase damping [6, 7]

$$\hat{E}_k = \sum_{l=0}^{D-1} \frac{(l\sqrt{-2\ln\eta})^k \eta^{l^2}}{\sqrt{k!}} |l\rangle \langle l|_c \otimes \mathbb{1}_w \quad (5)$$

with $\eta \in [0, 1]$ the strength of the phase damping [8]. By taking the parameterisation $\eta = e^{-\gamma t}$ with γ the probability of a phase error, we can say that the effect of the channel is weak (strong) for $\eta \rightarrow 1$ ($\eta \rightarrow 0$). We have introduced the orthonormal basis $\{|l\rangle_c\}$ spanning the coin space only, and $\mathbb{1}_w$ as the identity operator for the walker. We assume an initial coin-walker state decomposed as [6, 7]

$$\rho_{cw}(0) = \sum_{l,l',x,y} \rho_{l,x,l',y} |l\rangle \langle l'|_c \otimes |x\rangle \langle y|_w, \quad (6)$$

where we have introduced the orthonormal basis $\{|x\rangle_w\}$ spanning the walker space, and the coin-walker density matrix elements $\rho_{l,x,l',y} = {}_{c,w}\langle l, x | \rho_{cw}(0) | l', y \rangle_{c,w}$. Eq. (6) evolves under the action of the phase-damping channel on the coin space as

$$\mathcal{E}'[\rho_{cw}(0)] = \sum_{l,l'=0}^{D-1} \sum_{x,y} \rho_{l,x,l',y} \eta^{(l-l')^2} |l\rangle \langle l'|_c \otimes |x\rangle \langle y|_w. \quad (7)$$

In what follows, by simulating a process such that, for each walk, we select a value of η , apply the channel to the density matrix of the system after each time step of the walk, and evaluate the probability to reach a given vertex of the graph, we compare the behavior of the walks affected by phase damping ($0 < \eta < 1$) to what is found for an ideal walk (corresponding to $\eta = 1.0$).

In order to grasp the temporal behavior of the walk, we consider the change in the probability distribution of the walker's position on the graph at time t . In Fig. 2 we illustrate such a probability distribution for an ideal 25-step walk on the GT graph $G'6$. The target vertex (vertex number 253) is reached on step 15 with the highest probability (as shown by the large blue spike). In order to aid comprehension, we will now focus on the probability of the walker being on particular vertices on

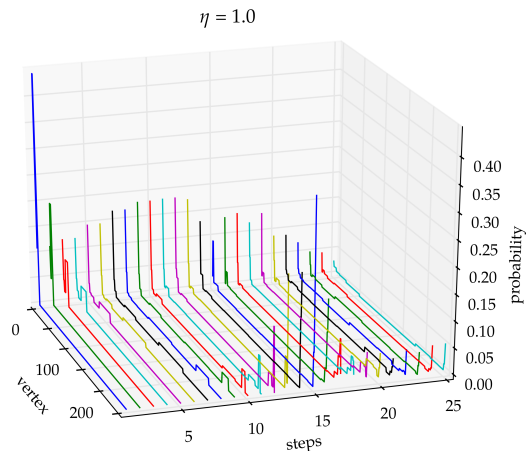


FIG. 2: How the probability that the walker is on specific vertices changes over time for the ideal walk (the walk unaffected by decoherence)

the graph and the overall vertex probability distribution for specific time steps.

In [9], the effect of decoherence on the walk on the hypercube was studied quantitatively. Starting from one corner, a decohered walker will reach the opposite corner in less time than in the ideal walk, hence highlighting a counterintuitive beneficial effect of such an incoherent process. Our goal here is to address similar questions for the walk on a GT graph as well, so as to investigate the limits of validity of the claim made in [9], where a lingering effect of a decohered walk on the target vertex was suggested. We will thus look for the possibility that a decohered walk reaches the target vertex in less steps than the ideal one, and also attempt to determine whether it remains on the target vertex for a longer time than in the ideal walk.

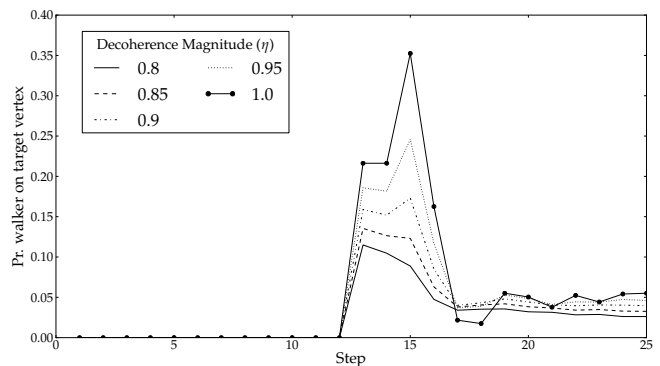


FIG. 3: Probability of walker being on target vertex per step for range of decoherence magnitudes.

III. DISCUSSION OF RESULTS

Here we present and discuss the results of our analysis, showing the behavior of walkers affected by decoherence of variable magnitude. All the results discussed in this Section were generated by simulating the previously discussed discrete-time reformulation of the Childs algorithm on the GT graph $G'6$.

In Fig. 3 we plot how the probability of the walker being on the target vertex changes over time for various decoherence magnitudes, ranging from the ideal walk with $\eta = 1.0$ to a decohered walk of $\eta = 0.8$. We see from this plot that the ideal walk takes 13 steps to achieve its goal of reaching the target vertex, where we say that the walker has reached some vertex v on some step of the walk t when there is a non-negligible probability of the walker being on v on the t^{th} time step. We see the ideal walk first appear on the target vertex on step 13 with probability $P \approx 0.216$, then remain or “linger” on the target vertex with non-negligible probability for 4 steps. The probability comes to a peak on step 15 with a value $P \approx 0.352$ before steadily decreasing. We henceforth refer to the probability that a walk is on some vertex v at a time step t as v 's *vertex probability* at time step t . We see in Fig. 3 that as η decreases, the target vertex probability steadily decreases. We see the peak on step 15 decrease at a faster rate than the target vertex probabilities associated with steps 13, 14 and 16. We note that for $\eta = 0.8$ and $\eta = 0.85$ the target vertex probability is higher on step 13 than on step 15. If the value of decoherence magnitude was known a priori to be $\eta \approx 0.8$ then it would be most effective to run the walk for 13 time steps only.

Some interesting behavior can be observed on steps 17 and 18 of the walk. We observe that decoherence magnitude $\eta < 1.0$ slightly increases the target vertex probability, or in other words, the ideal walk is less likely to be on the target vertex on steps 17 and 18 than the decohered walks. This behaviour was reported in [9]. The effect can be seen more clearly in Fig. 4, in which we plot the effect of decoherence on the target vertex probability on various steps of the walk. As can be seen in the curves for steps 17 and 18 in Fig. 4, the target vertex probability is higher for walks affected by decoherence of magnitude $\eta < 1.0$, with the probability peaking at $\eta \approx 0.9$. This is an effect of decoherence spreading out the range of time steps over which the target vertex probability is significantly larger than the classical value. In line with the claims in [9], we have indeed seen that weak decoherence increases the probability for the extended number of time steps. However, the difference between the target vertex probabilities of the ideal walk and the walk with decoherence magnitude $\eta = 0.9$ on steps 17 and 18 is very small, we see an increase of approximately 0.026.

Fig. 4, as previously discussed, is a plot of the effect of decoherence on the target vertex probability on various time steps. The curve representing step 15 illustrates the effect of decoherence very well, and confirms the results

reported in [9], as the decoherence magnitude η decreases the target vertex probability decreases exponentially: in other words, the Childs algorithm becomes exponentially less effective at achieving its goal as η decreases.

We shall now investigate the extent of the “damage” that decoherence has on the Childs algorithm’s effectiveness. We concede that as long as the target vertex probability is higher than the other vertex probabilities then the decoherence has not had a particularly damaging effect on the effectiveness of the Childs algorithm i.e. if phase damping decreased the peak associated with the target vertex below the other probability peaks then the algorithm would end up in a state involving a more probable “false-positive” than a “positive” when affected by decoherence – we would say that this is a serious blow to any algorithm’s usefulness. In Fig. 5 we have plotted the entire graph’s vertex probabilities on step 15 (the step on which, as previously mentioned, the probability of the walker being on the target vertex was the highest for most values of η) of walks with various decoherence magnitudes. When the chosen target vertex is number 253 on the graph, we see that the probability is always higher than the non-target vertex probabilities, regardless of the value of η . In Fig. 6, we illustrate this behavior more clearly by magnifying the trends associated with three different groups of vertices in the graph $G'6$.

With Fig. 7 we can get a clearer picture on how the probability peaks change in the walks affected by decoherence. In order to improve the legibility of the plot while maintaining the number of shown vertex probabilities at an acceptable level, we present only the vertex probabilities $P > P_t/4$ where P_t is the target vertex probability. We can see that in steps 13 to 16 of the walk, the peak representing the target vertex probability never drops below any of the other vertex probability peaks. We find this significant and can conclude from it that the Childs algorithm is not affected to the extent previously described: the walk is never on a non-target vertex with greater probability than the target vertex when allowed to run for sufficient time and phase damping decoherence does not change this fact.

The authors of [9] investigate the evolution of a discrete time quantum walk on the hypercube using a Grover coin. They plot the probability that the walk is on a target vertex (they begin the walk on a corner of the hypercube and take the target vertex to be the vertex in the opposite corner of the hypercube) for a number of time steps, in the same way we have done in this paper. They observe that decoherence lowers the probability peaks of their plots in the same way that it does in our plots regarding the walk on the glued trees graphs, but they also observe that the “troughs” in their plots (sections of the curve representing vertices with probability much lower than others) become raised when decoherence is applied to a walk. This same effect can be observed in the walks we simulated on the glued trees graphs and can be seen in Fig. 5, and more clearly in Fig. 6, where vertex numbers in the approximate range 10-240 have their probabilities

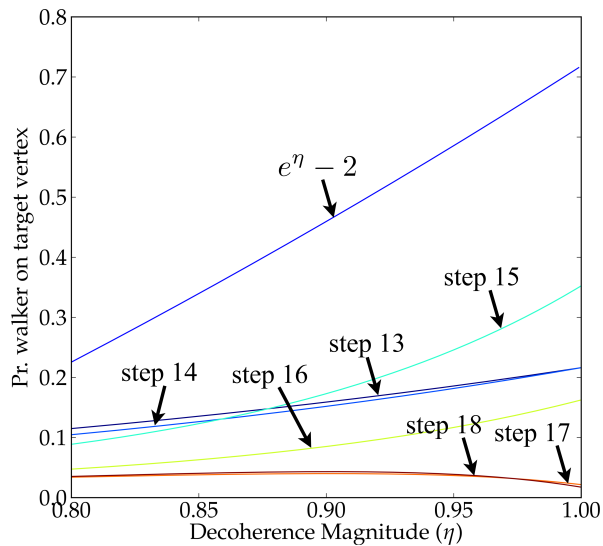


FIG. 4: Probability of walker being on target vertex over decoherence magnitude for range of step numbers. Exponential function plotted for comparison.

boosted slightly by the decoherence, with the lowest decoherence magnitude we investigated, $\eta = 0.8$, raising the probability by the greatest amount.

IV. CONCLUSIONS

In this paper we discussed a discrete time reformulation of the continuous time quantum walk algorithm described by Childs *et al.* in [1]. We simulated this discrete time walk on GT graphs and applied phase damping to the coin space of the walk, in order to study the algorithm's resilience to decoherence. We did this by studying how effectively it achieved its goal when affected by decoherence of various magnitudes: we investigated how decreasing the decoherence magnitude η (making the decoherence "stronger") lowered the probability of the walker being on the target vertex at the end of the

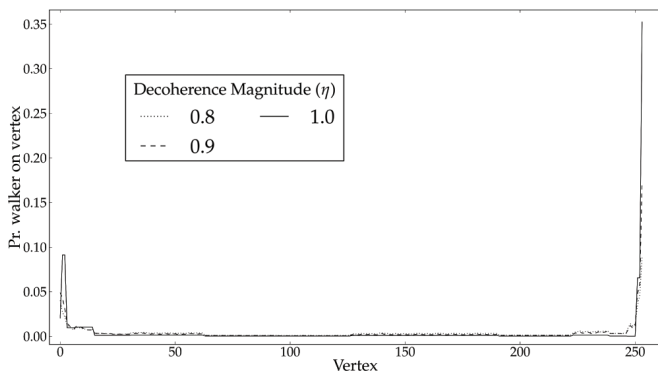


FIG. 5: Change in vertex probabilities on step 15 for range of decoherence magnitudes.

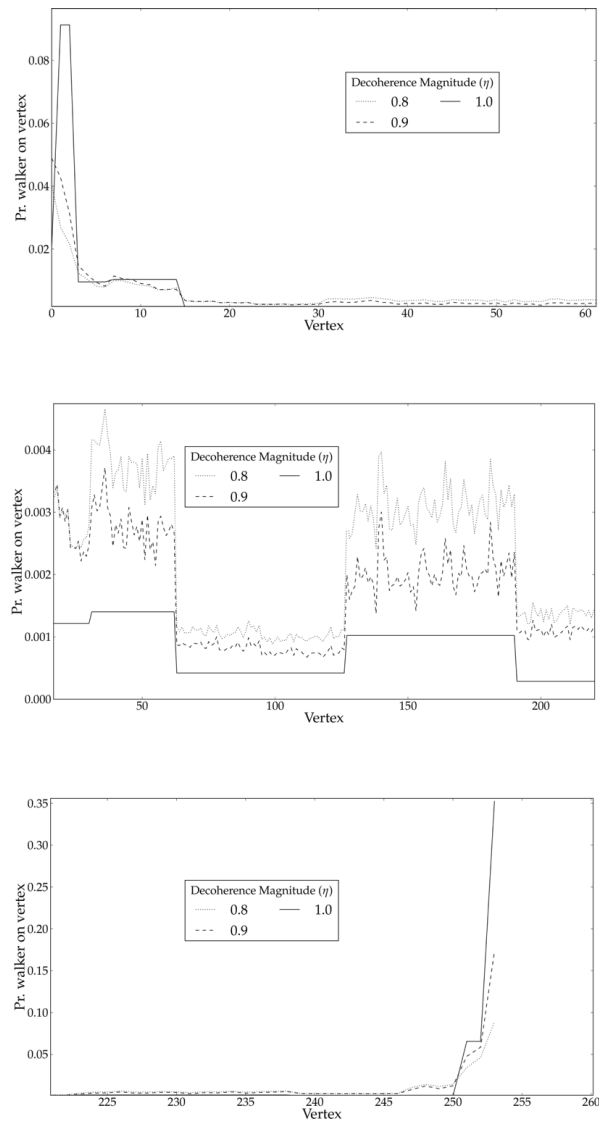


FIG. 6: Change in vertex probabilities on step 15 for range of decoherence magnitudes. Note that each plot has different vertex numbers on the x-axis.

walk. We first simulated the walk with no decoherence to find how many steps the walk took to reach the target vertex (we say that the walk has reached a vertex when the probability that the walk is on the vertex is non-negligible). We then included a range of decoherence magnitudes $0.8 \leq \eta < 1.0$ to see the extent of the drop in the target vertex probability at the end of the walk.

We observed that the ideal walk found the target vertex at time step 13 and remained there with non-negligible probability until time step 16. We found that strengthening the decoherence (decreasing η) lowered the target vertex probability on time steps 13 to 16, but that the target vertex always had a higher probability than any other vertex, regardless of decoherence magnitude. We also observed that a decoherence magnitude

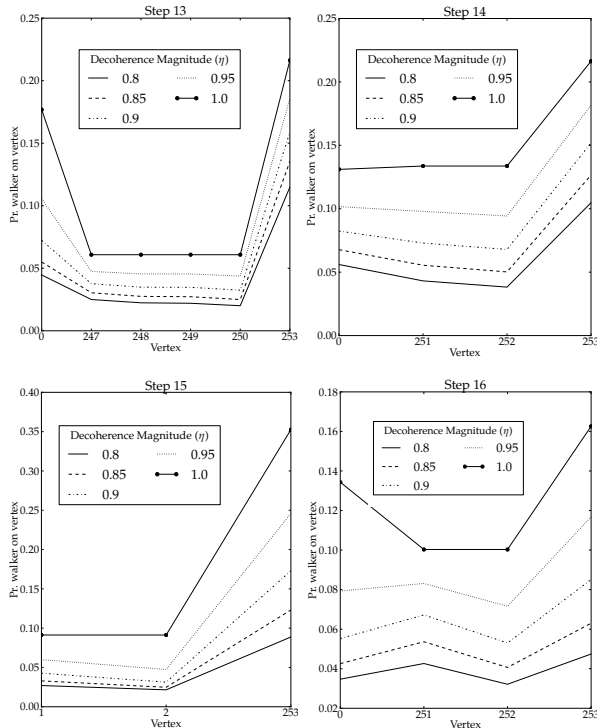


FIG. 7: Target probability peaks compared to other peaks on step 13 to 16.

of $\eta \approx 0.9$ boosted the target vertex probability very slightly on steps 17 and 18. Finally, we found that ver-

tices with very low probabilities had their probability of being reached by the walker boosted slightly by decoherence.

Our results have touched on some unexplored features of the Childs algorithm on GT graphs, in turn opening up new questions to address. The first of such behaviours is the rate at which the target vertex probability on time step 15 decreases with η : out of the time steps 13-16, step 15’s target vertex probability decreases at the highest rate. The second unexplained behaviour is observed in steps 17 and 18 of the walks studied in this paper. When compared to the target-vertex probability for the ideal walk, we see a slight increase of 0.026 in the target-vertex probability for $\eta = 0.9$. Finally, the boosting of the troughs in Fig. 5 by decoherence. This boosting of the troughs by decoherence appears to be a similar phenomenon to the boosting of the target-vertex probabilities in steps 17 and 18.

Our results add more weight to the claims made in [9] on decohered walks: the “lingering” effect of the decohered walkers is shown to be only marginally relevant because the boost in probability for the two steps after the target vertex probability drop (steps 17 and 18) caused by the decoherence is very small. On the other hand, we have observed that decoherence does not cause any upset to the notion that at the end of the walk, the walker should be on the target vertex with a higher probability than any other vertex.

Acknowledgments

This work has been supported by the UK EPSRC through a Career Acceleration Fellowship, a grant under the “New Directions for Research Leader” initiative (EP/G004579/1), and the equipment grant (EP/K029371/1). JL thanks the Centre for Theoretical Atomic, Molecular, and Optical Physics for hospitality during the early stages of this work.

-
- [1] A. M. Childs, R. Cleve, E. Deotto, E. Farhi, S. Gutmann, and D. A. Spielman, STOC ‘03, Proc. 35th ACM Symposium on Theory of Computing, 59 (2004).
 - [2] M. A. Nielsen, and I. L. Chuang, *Quantum Computation and Quantum Information* (Cambridge University Press, 2000).
 - [3] B. Tregenna, W. Flanagan, R. Maile, and V. Kendon, New J. Phys. **5**, 83 (2003).
 - [4] J. Kempe, Contemp. Phys., **44**, 307 (2003).
 - [5] A. Ambainis, E. Bach, A. Nayak, A. Vishwanath, and J. Watrous, STOC ‘01, Proceedings of the 33rd annual ACM symposium on Theory of computing, 37 (2002).
 - [6] Y. Liu, A. K. Özdemir, A. Miranowicz, and N. Imoto, Phys. Rev. A **70**, 042308, (2004).
 - [7] S. Pirandola, S. Mancini, S. L. Braunstein, and D. Vitali, Phys. Rev. A **77**, 032309 (2008).
 - [8] G. Amosov, S. Mancini, and V. Manko, J. Phys. A: Math. Gen. **39**, 3375 (2006).
 - [9] V. Kendon, and B. Tregenna, Phys. Rev. A **67**, 042315 (2003).